Biochimica et Biophysica Acta xxx (2010) xxx–xxx

Contents lists available at ScienceDirect

Biochimica et Biophysica Acta

journal homepage: www.elsevier.com/locate/bbagen

Small-angle X-ray scattering studies of the intact eye lens: Effect of crystallin composition and concentration on microstructure

Amir Y. Mirarefi [a], Sébastien Boutet [b], Subramanian Ramakrishnan [c,*], Andor J. Kiss [d], Chi-Hing C. Cheng [e], Arthur L. DeVries [e], Ian K. Robinson [b], Charles F. Zukoski [a]

[a] Center for Biophysics and Computational Biology in the Department of Chemical and Biomolecular Engineering, University of Illinois at Urbana-Champaign, Urbana, IL 61801, USA
[b] Department of Physics, University of Illinois at Urbana-Champaign, Urbana, IL 61801, USA
[c] Department of Chemical and Biomedical Engineering, FAMU-FSU College of Engineering, Tallahassee, FL 32310, USA
[d] Laboratory for Ecophysiological Cryobiology, Department of Zoology, Miami University, Oxford, OH 45056, USA
[e] Department of Animal Biology, University of Illinois at Urbana-Champaign, Urbana, IL 61801, USA

ARTICLE INFO

Article history:
Received 6 August 2009
Received in revised form 4 February 2010
Accepted 8 February 2010
Available online xxxx

Keywords:
Crystallin
Lens
Liquid–liquid phase separation
Transparency
Short-range order
Small-angle X-ray scattering (SAXS)
Antarctica

ABSTRACT

Background: The cortex and nucleus of eye lenses are differentiated by both crystallin protein concentration and relative distribution of three major crystallins (α, β, and γ). Here, we explore the effects of composition and concentration of crystallins on the microstructure of the intact bovine lens (37 °C) along with several lenses from Antarctic fish (−2 °C) and subtropical bigeye tuna (18 °C).
Methods: Our studies are based on small-angle X-ray scattering (SAXS) investigations of the intact lens slices where we study the effect of crystallin composition and concentration on microstructure.
Results: We are able to distinguish the nuclear and cortical regions by the development of a characteristic peak in the intensity of scattered X-rays. For both the bovine and fish lenses, the peak corresponds to that expected for dense suspensions of α-crystallins.
Conclusions: The absence of the scattering peak in the nucleus indicates that there is no characteristic wavelength for density fluctuations in the nucleus although there is liquid-like order in the packing of the different crystallins. The loss in peak is due to increased polydispersity in the sizes of the crystallins and due to the packing of the smaller γ-crystallins in the void space of α-crystallins.
General significance: Our results provide an understanding for the low turbidity of the eye lens that is a mixture of different proteins. This will inform design of optically transparent suspensions that can be used in a number of applications (e.g., artificial liquid lenses) or to better understand human diseases pathologies such as cataract.

1. Introduction

The vertebrate eye lens is a transparent tissue composed of fiber cells arranged in a concentric onionlike fashion devoid of cellular organelles populated by a dense assortment of three types of crystallin proteins [1,2]. The density of the fiber cells and the crystallins therein is maximal at the center of the lens and least dense at the periphery of the lens where newly formed fiber cells are constantly being added by the lens epithelial layer [3]. Vertebrate crystallins are found as three types (α, β, and γ) based on their size, sequence, and immunoreactivity [2]. α-Crystallin is a large polydisperse oligomer with as many as 32 subunits having a molecular weight ranging between 700 and 1200 kDa, whereas β-crystallin can be isolated as smaller oligomeric β_H (high) and β_L (low) crystallins (50–300 kDa) [2]. The smallest of the three (α, β, and γ) are the monomeric γ-crystallins (~20 kDa). Crystallins are commonly isolated from lens homogenates by size exclusion chromatography (SEC) resulting in some aggregation generating polydispersity in their hydrodynamic diameters. The aggregation seen with α-crystallin varies from investigator to investigator likely owing to different resins and animals (age and taxa) used. For example, mammalian α-crystallin coisolates with minor amounts of β_H-crystallin, whereas fish α is aggregated with substantially more β_H-crystallins [4].

When isolated crystallins are measured using dynamic light scattering (DLS), α/β_H and β_L proteins have modal sizes of 23 nm and 15 nm, respectively [5]. γ-Crystallins have a narrow size distribution with an average hydrodynamic diameter of 5.5 nm. Both total protein concentration and proportion of γ-crystallins in vertebrate lenses increase moving inward from cortex to nucleus. The variation in both total concentration as well as crystallin composition (increased γ-crystallin) across the eye lens generates a significant protein gradient, which contributes to the refractive index of the lens [6]. Little is known about the *in vivo* spatial arrangement of the crystallins and how they vary between the lens cortex and nucleus.

* Corresponding author. Tel.: +1 850 410 6159; fax: +1 850 410 6150.
E-mail address: srama@eng.fsu.edu (S. Ramakrishnan).

0304-4165/$ – see front matter © 2010 Elsevier B.V. All rights reserved.
doi:10.1016/j.bbagen.2010.02.004

However, measurements with small-angle X-ray scattering (SAXS) suggest that while a regular spacing between particles could be largely attributed to the α-crystallin [7–9], it remains unknown if the spatial arrangement of crystallins differs between the cortex and nuclear region of the lens. In addition, no study has been done on animals whose lenses are extremely dense (≥900 mg ml^{-1}) such as fish [10,11] that have dramatically higher γ-crystallin content than terrestrial mammals [5,12,13].

Transparency in the eye lens has been hypothesized to result from spatial short-range ordering of crystallins [7,14,15]. Usually, ordering is associated with density variations that are periodic and thus have a characteristic wavelength or separation length, d. The existence of a regular spacing is typically demonstrated through the existence of peaks in the angular dependence of the intensity of X-rays scattered from a sample. Peaks are observed at a wave vector $q = 2\pi/d$ where $q = (4\pi/\lambda)\sin(\theta/2)$ with λ being the wavelength of the X-rays and θ, the scattering angle. However, unlike crystalline order in which particles (atoms or molecules) comprising a crystal are placed on a regular lattice, particles in the lens are in a liquid-like order that pack in an amorphous noncrystalline structure. The spacing between particles in this structure is much less regular than in a solid crystal. Consequently, in such concentrated systems, the periodicity of the density variations has a wavelength that approaches the order of the particle size. Thus, in a concentrated solution of proteins of diameter σ, the characteristic spacing is of the order of σ, which gives rise to density fluctuations with a wavelength of $\sim 2\pi/\sigma$. When probed by X-ray scattering (SAXS), these density fluctuations give rise to a scattering peak at $q = 2\pi/\sigma$. DLS studies on intact mammalian lenses suggest that despite protein concentrations as high as 400 mg ml^{-1} corresponding to protein volume fractions of $\phi = 0.29$ (assuming the protein density = 1.35 g ml^{-1}), proteins still have substantial mobility and diffuse at rates characteristic of sizes expected from SEC-fractionated proteins [16–18]. These studies would indicate that order within the mammalian lens is indeed liquid-like arising from amorphous packing of crystallins that are free to diffuse over relatively large distances when contrasted to their size.

Fish eye lens are known to have a much higher protein concentration than terrestrial mammals [6,10,19,20]. Our preliminary studies suggested crystallin proteins in these lenses have very limited mobility indicative of nonergodic or gelled states [21]. Lack of mobility may be associated with the high-volume fractions that act to limit long-range diffusion (macromolecular crowding) and/or alternatively attractive interactions that localize and aggregate crystallins. The microstructure of gelled systems is less well characterized and depends both on the nature of the attractive interactions giving rise to the gel as well as the volume fraction of particles within the gel [22,23]. Moreover, owing to the extremely high concentration of crystallins in fish lens and owing to the volume exclusion of proteins of diameter σ, we would expect density variations with a wavelength on the order of $2\pi/\sigma$.

In this report, we have investigated the X-ray scattering properties of the crystallins within intact cortex and nuclear slices of the eye lens of both terrestrial mammals and fish. By examining the spatial distribution of the X-ray scattering elements (crystallins) within intact lens fiber cells, we explore the *in situ* spatial arrangement of the crystallins in their native environment without the complications (aggregation, oxidation, and precipitation) encountered in previous reports introduced by disrupting the lens [7,8,15,24]. We report SAXS observations from the intact lens of five animal species showing a characteristic spacing in the cortex consistent with scattering from a dense suspension of α/β_H-crystallins. In all species, this characteristic spacing was absent in lens nucleus. To our knowledge, this is the first report of a direct measurement in intact lens tissue demonstrating the loss of this characteristic peak, suggesting there are structural, or physical, differences of the crystallin arrangement between the cortex and nuclear regions of the lens. We propose that this loss of a characteristic peak can be attributed to both changes in size distribution (composition) of the crystallins in the cortex when contrasted to those in the nucleus, along with packing of the smaller γ-crystallins in the void space of the larger α/β-crystallins.

2. Materials and methods

Lenses from adult Antarctic toothfish *Dissostichus mawsoni*, *Trematomus bernacchii*, and *Pagothenia borchgrevinki* were obtained from live specimens caught in McMurdo Sound, Antarctica. Adult bigeye tuna (*Thunnus obesus*) lenses were a generous gift of Timothy Ke (Luen Thai Fishing Venture, Ltd., Hong Kong and LTFV-USA) from specimens caught off the coast of the Marshall Islands. Eight- to twelve-month-old calf (*Bos taurus*) lenses were obtained from Allen's Farm Quality Meats, Homer, Illinois, USA. Detailed separation methods and chromatographic profiles for bovine and fish lenses have been previously reported [5,25]. The relative concentrations of α, β, and γ proteins in lens vary between different animals, with fish lens showing a higher overall concentration richer in γ-crystallins (≥900 mg ml^{-1}) relative to most terrestrial mammals (~600 mg ml^{-1}) [19,20,26]. Mammalian eye lens proteins exist in the lens at concentrations of ~250 mg ml^{-1} in the outer cortex corresponding to a protein volume fraction $\phi = 0.185$, and increase in concentration to ~400 mg ml^{-1} in the nuclear region corresponding to $\phi = 0.29$. Values previously measured for both cow [15] and fish [5,11,25,27] will be used as a guide (Table 1) for representative relative concentrations of the different crystallin classes in these animal taxa.

The small-angle X-ray scattering (SAXS) measurements were performed at sector 34ID-C of the Advanced Photon Source at Argonne National Laboratory (Argonne, IL, USA). A wavelength of 1.39 Å was selected from the radiation produced by the undulator using a double-crystal Si(111) monochromator. The beam obtained was collimated using two sets of slits located 1500 mm and 10 mm upstream of the sample. The scattered X-rays were detected using a direct-read Roper Scientific CCD camera with 20 μm pixels located 1004 mm from the sample. The exposure time varied for each sample to prevent detector saturation but was typically on the order of 50 seconds.

The scattered intensity, $I(q)$ was measured for the thin slices of lenses of the bovine and several Antarctic fish. The limited penetration depth of the X-rays into the sample made it necessary to use thin slices rather than whole lenses. The thickness of the slice only affects the scattered intensity by multiplying the whole curve by a constant in the kinematical approximation (ignoring multiple scattering),

Table 1
Lens crystallin composition, protein density, volume fraction of species used in this study and d spacing as measured by X-ray scattering. Mean composition [5] of the *B. taurus* and *D. mawsoni* are also given in the table. The crystallin composition of the other fish species is expected to be similar to that of *D. mawsoni* [10,11,54,55]. The mean crystallin composition in the cortical and nuclear regions for species is approximated from literature [28,54] and direct measurements [28]. A density of 1.35 g ml^{-1} is used to convert concentrations to volume fractions (ϕ) [56].

	Mammalian (terrestrial)	Fish (aquatic)
Species	*B. taurus*	*D. mawsoni*, *T. obesus*, *P. borchgrevinki*, *T. bernacchii*
Crystallin composition (%)	α/β_H 54 β_L 27 γ 19	α/β_H 52 β_L 5 γ 43
Mean [crystallin] cortical region	250 mg ml^{-1} ($\phi \sim 0.2$)	450 mg ml^{-1} ($\phi \sim 0.33$)
Mean [crystallin] nuclear region	600 mg ml^{-1} ($\phi \sim 0.44$)	800 mg ml^{-1} ($\phi \sim 0.59$)
d spacing as measured by X-ray scattering[a] (nm)	17	14, 13, 12, and 15, respectively

[a] The *d* spacing as measured by X-ray scattering can be measured to within 0.04 nm^{-1} in q space which translates to less than 10% error in *d* spacing.

Please cite this article as: A.Y. Mirarefi, et al., Small-angle X-ray scattering studies of the intact eye lens: Effect of crystallin composition and concentration on microstructure, Biochim. Biophys. Acta (2010), doi:10.1016/j.bbagen.2010.02.004

which we assume to hold in this analysis. However, if the sample was too thin, the scattering would have been too low to measure, and if the sample were too thick, the X-rays would have all been absorbed and no signal is seen. Thus, the ideal situation is to have a sample that has the thickness corresponding to the extinction length of the material, which is the length through which $1/e$ of the incoming beam is absorbed, where e is the base of the natural logarithm. This tends to maximize scattering while keeping absorption within the range of the detector. For aqueous samples (and by approximation, biological cells), this extinction length is 1 mm. The lens slices were made approximately 1 mm in thickness and were taken to include the diameter of the fish lenses or the largest chord of the cow lenses. We defined the inner third of the lens as the nuclear region, or nucleus, while the remaining outer two–thirds referred to as the cortex. The 1-mm slices were placed between two thin kapton windows and mounted on a custom-made holder, which was then mounted to a Peltier cooler using thermal paste allowing temperature to be varied between −20 °C and +40 °C. Using direct physical measurements in this study, it is difficult to distinguish between the α- and α/β_H-crystallins on the basis of size, owing to their intimate association, especially in fish [28,29]. As a result, we will discuss X-ray and dynamic light scattering (DLS) in terms of three fractions, α/β_H-, β_L-, and γ-crystallins. The collected CCD images were integrated using the Fit2D program (http://www.esrf.eu/computing/scientific/FIT2D/).

Normalization of the scattered intensities was done by fitting the data at high q to $I \sim I_0\ (Aq^{-4}+B)$ [28]. I_0 is the intensity of the incoming X-ray normalized by the sample absorbance and the path length of the X-rays through the sample. As discussed by Wagner et al. [30], in the high q limit for particles with sharp interfaces, the particle form factors decay as q^{-4} (Porod's Law), while the structure factors will all reach unity. The background value, B, arises from random noise, and this was subtracted from the data. Owing to minor path length variations in the lens slices, I_0 will be proportional to $\exp(-al)$ where a is the sample absorbance and l is the path length the X-rays have to travel through the sample. For the intact lens slices, we varied the location of the beam to minimize the effect of an extended exposure of the sample to the X-ray beam, which quickly damages biological samples. This changed l slightly for different temperatures where we reported scattering measurements. As a result, normalization of the scattered intensities at high q produced a plot where we took into account variations in concentration and path length. In the data given (see results below), we always report results normalized at the highest q measured. Also, the performed normalization does not affect the scattering at low q and intensities around the peak of the scattering curve. Whether it be the nucleus or cortex, intensities at the highest q measured ($1\ \mathrm{nm}^{-1}$) should obey Porod's Law, and this is taken care of in the normalization procedure.

3. Results

3.1. Scattering from the cortex region of the eye lens

Periodic variations in density can be measured by the peaks in the scattered intensity which occur at $q \sim 2\pi/d$, where d is a measure of distance between concentration maxima. Local spatial order of crystallins is expected to be seen as peaks in the total intensity of scattered X-rays. However, interpretation of X-rays scattered from intact lens slices can be complicated by the presence of multiple populations of crystallins of varying sizes that contribute to the total observed scattering. Thus, there exists the likelihood that the total scattering is a combination of different form factors and partial structure factors [31–34]. To parse this complex signal, we measure total scattered intensity and analyze data pertaining to periodic spacing between the principal and major scattering elements.

The scattering from the intact cortex of a calf lens was measured at different temperatures (Fig. 1a). At all temperatures, the scattered

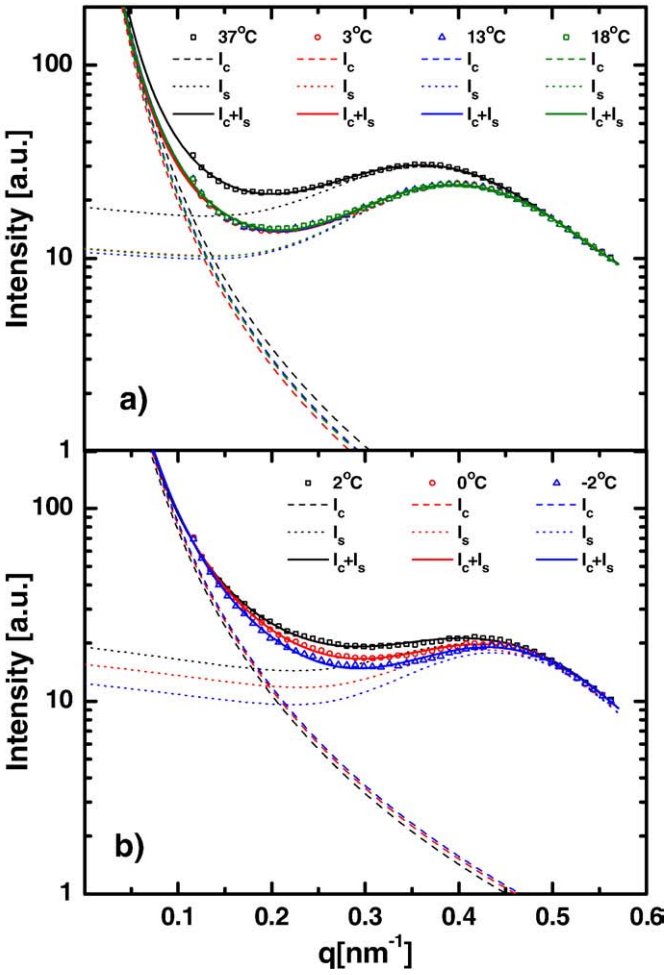

Fig. 1. (a) Integrated SAXS intensity measured on slices of bovine cortex. The curves were all scaled so that the intensity at the highest q value measured was the same for all curves. The peak position varies from $q = 0.4\ \mathrm{nm}^{-1}$ at temperatures below 18 °C to $q = 0.36\ \mathrm{nm}^{-1}$ at 37 °C. This corresponds to a change in spacing from 16 nm to 18 nm. (b) The scattering intensity from the intact cortex of a *D. mawsoni* lens. The peak position varies from $q = 0.45\ \mathrm{nm}^{-1}$ at −2 °C to $q = 0.41\ \mathrm{nm}^{-1}$ at 2 °C. This corresponds to a change in spacing from 14 nm to 15 nm. In all cases, the symbols are the measured data, the dashed lines are I_c as fitted using Eq. (1), the dotted lines are the I_s values obtained from subtracting I_c from the data and the solid lines are the total fit of $I_c + I_s$.

X-ray intensity shows a peak between $q \sim 0.36$ and $0.40\ \mathrm{nm}^{-1}$ suggesting periodic density fluctuations of $d = 16$–18 nm. In addition, in the low q region, there is an upturn in scattered intensity (Fig. 1a). Upturns at low q are usually indicative of density fluctuations at that characteristic length. The question is how one gets to these fluctuations. The physics in the current work assumes that these are due to the particles wanting to get closer together and this arises from attractions between the particles. Research has shown that, attractive interactions are expected to play important effects in binary mixtures of α and γ proteins, and it is expected to find clusters of proteins in the eye lens [35–38]. To back out an average cluster size, the total scattered intensity is modeled as composed of scattering from clusters of dense spheres and scattering from the crystallins.

$$I_c(q) = \left(\frac{I(0)}{\left[1 + ((q\xi)^2)\right]^{(d_f-1)/2}}\right)\frac{\sin\{(d_f-1)\tan^{-1}(q\xi)\}}{(d_f-1)q\xi} \quad (1)$$

where ξ is the radius of the clusters and d_f is the fractal dimension. Assuming the low-angle scattering arises from a dilute suspension of

Please cite this article as: A.Y. Mirarefi, et al., Small-angle X-ray scattering studies of the intact eye lens: Effect of crystallin composition and concentration on microstructure, Biochim. Biophys. Acta (2010), doi:10.1016/j.bbagen.2010.02.004

dense clusters ($d_f \sim 3$) and a characteristic size, $\xi \sim 50$ nm, we demonstrate a fit to the low q data for each temperature (Fig. 1). The hypothetical fit to Eq. (1) (I_c) is shown as a dashed line for each temperature in Fig. 1. There is a limited range of q where the scattering from the clusters dominates the observed data, which results in large uncertainties in cluster size. Thus, a cluster size of 50 nm should be taken as a guide to the size of the clusters that exist in the native eye lens. Given the dilute concentration of the 50 nm clusters, we follow Shah et al. (2003) and approximate the scattering from the eye lenses as being composed of the sum of scattering from a dilute suspension of clusters and individual crystallins:

$$I(q) = I_c(q) + I_s(q) \quad (2)$$

where $I_s(q)$ is the scattering from the crystallins [23]. We show the scattering $I_s(q)$ as a dotted line where we have subtracted from the total scattered intensity the value of $I_c(q)$ as determined by Eq. (1) with $\xi = 50$ nm and $d_f = 3$ (Fig. 1). This representation of the data emphasizes the peak in $I_s(q)$ and shows that $I_s(q)$ approaches a constant value (within our ability to measure) at low q. Solid lines in Fig. 1 represent the total scattered intensity, which is the sum of scattering from clusters (I_c) and scattering from the individual crystallins (I_s). It should also be mentioned here that in the calculation of an average cluster size, a detailed multicomponent model, taking into account attractions between the different crystallins, was not developed. Such a model if developed will give detailed information as to composition of these clusters and the strength of attractions between different crystallins when compared with experimental data. Thus, as mentioned before, a cluster size of 50 nm should be just taken as a guide to the size of the clusters that exist in the native eye lens.

In Fig. 1a, the observed peak in $I(q)$ moves from $q = 0.36$ nm^{-1} at 37 °C to $q = 0.40$ nm^{-1} for $T \leq 18$ °C after which the scattered intensity is independent of temperature. This shift in q corresponds to d shifting from 18 to 16 nm. The bovine lens nucleus begins to opacify through a liquid–liquid phase separation beginning at a temperature ~18 °C, suggesting that our observed shift in the peak position and the magnitude may be associated with phase separation in these systems. If the scattering in the cortex were dominated by a single, nondeformable species, the increase in q at the maximum would indicate that the particles are moving into a closer packed state with core diameters of 16 nm.

As in the bovine system, there is a peak in the Antarctic toothfish cortex associated with the α/β_H-crystallins (Fig. 1b). This peak occurs at $q = 0.42$–0.43 nm^{-1} and the shift to larger q with decreasing temperature is not as strong as in the bovine case (Fig. 1a). The larger value of q at the peak indicates protein density fluctuations with a characteristic wavelength of 14 to 15 nm. The upturn in scattering at small angles is consistent with the presence of a low concentration of dense objects with a characteristic size of ~50 nm. We show the intensity $I_s(q)$ with $I_c(q)$ subtracted in Fig. 1b. The shift in peak position to higher values of q is also consistent with increased concentration of proteins in the toothfish (450 mg ml^{-1}; Table 1) than in the bovine system (250 mg ml^{-1}).

The scattered intensity from the cortical slices of three other species of fish is shown in Fig. 2. These include (A) *P. borchgrevinki* and (B) *T. bernacchii*, both of which are Antarctic notothenioids that live in the subzero (−2 °C) Southern ocean [39] and (C) bigeye tuna *T. obesus*, which is a subtropical fish that endothermically regulates its body temperature to a constant value of ~18 °C [40]. Each of these cortical lens samples shows a peak in intensity corresponding to a spacing of 12 nm, 15 nm, and 13 nm, respectively. We take the rapidly increasing intensity at low q as an indication of formation of larger clusters, previously observed with the bovine and toothfish samples (Fig. 1).

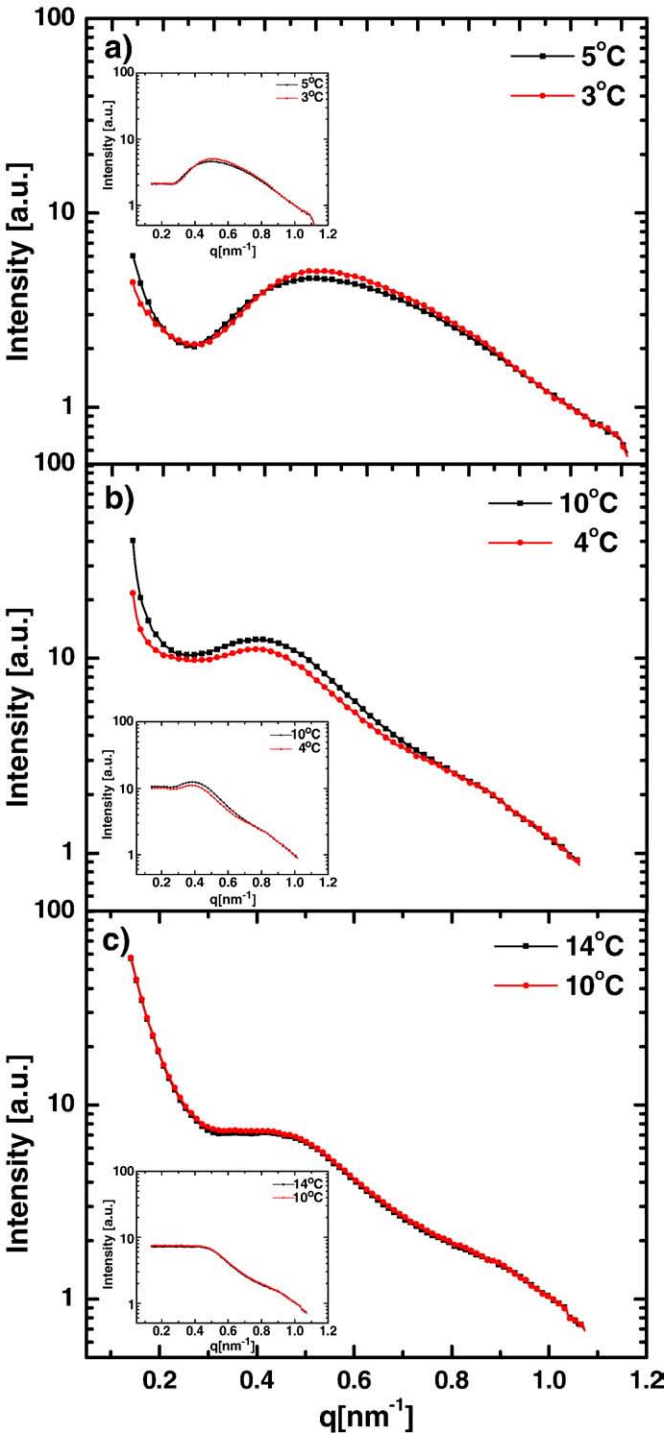

Fig. 2. (a) Integrated SAXS intensity measured on slices of *P. borchgrevinki* cortex. The peak position is at $q = 0.5$ nm^{-1}. This corresponds to a spacing of 12 nm. (b) The scattering intensity from the intact cortex of a *T. bernacchii* lens. The peak position is at $q = 0.43$ nm^{-1} which corresponds to a spacing of 15 nm. (c) Scattered intensity from the intact cortex of *T. obesus*. The peak is at $q = 0.47$ nm^{-1} which corresponds to a spacing of 13 nm. Insets show the intensity from the protein suspension after subtraction of the contribution from larger clusters.

3.2. Scattering from the nuclear region of the eye lens

The scattering from the nuclear region of the bovine and fish lenses was also investigated (Fig. 3). Although the water content in the nucleus is less than that in the cortex thus leading to a reduced water contrast, the measured scattering signal was strong indicating the particle dominance of scattering. Thus the effects seen in Fig. 3 are

Please cite this article as: A.Y. Mirarefi, et al., Small-angle X-ray scattering studies of the intact eye lens: Effect of crystallin composition and concentration on microstructure, Biochim. Biophys. Acta (2010), doi:10.1016/j.bbagen.2010.02.004

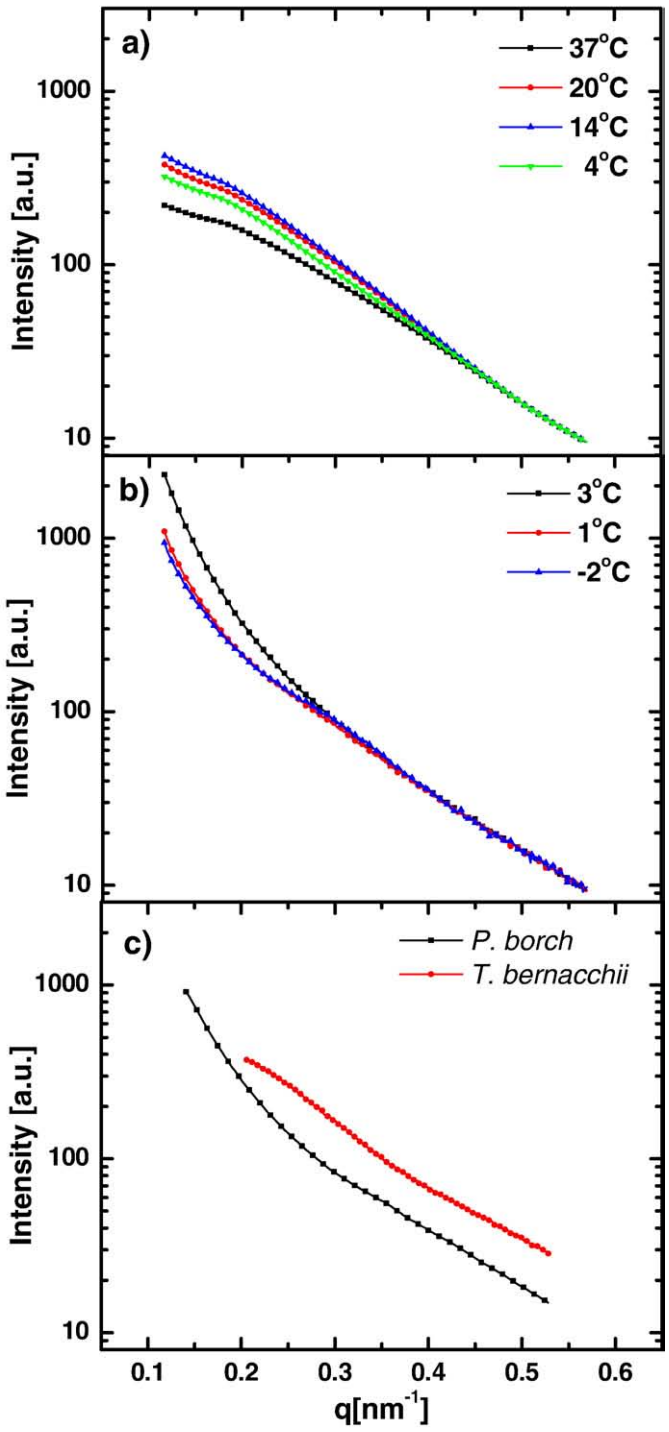

Fig. 3. (a) Integrated SAXS intensity from the nucleus of the bovine. (b) Scattering from the intact nucleus of a *D. mawsoni* lens. (c) Scattered intensity from the *P. borchgrevinki* and *T. bernacchii* nuclei at $T = 3$ °C.

real, and loss of peak is not due to reduced scattering intensities. Similar to scattering in the cortex, the data are normalized at high q to obey Porod's Law. Unlike scattering from the bovine nucleus (Fig. 3a), the scattered intensity in fish lens shows a monotonic decrease with increasing scattering angle (Fig. 3b). The lack of a peak in the scattering intensity suggests that there is no characteristic wavelength associated with regular density fluctuations in the q range characterized. For the bovine eye lens nucleus, lowering temperature increased the scattering at low q, while for the toothfish (*D. mawsoni*) raising temperature had a similar effect. While this effect in the bovine lens may occur due to the well-characterized liquid–liquid phase separation (LLPS) [41], increases in intensity at low scattering angle could also be attributed to increasing attractions between the particles that remain in a single phase [42]. For the Antarctic toothfish, no opacification (LLPS) is observed at temperatures as low as −12 °C or as high as 25 °C by visual inspection as previously described (for lens photographs, please see Kiss et al. [5]). However, it is important to consider that the toothfish has adapted to a stable environmental temperature of −2 °C for the past 10 ~ 20 million years [43]. Thus, one would expect toothfish protein instability and aggregation to be manifest at mammalian thermal norms (37 °C) that are 40 °C above its normal environmental (organismal) temperature. At high temperatures, the toothfish lens crystallins may be showing aggregation and coalescence indistinguishable from a cold-induced LLPS seen in the bovine lens as observed by SAXS.

4. Discussion

4.1. Suppression of density fluctuations and its relationship to transparency

Using a comparative approach, we have examined the scattering elements in the intact vertebrate lens cortex and previously unexamined scattering within the lens nucleus. Prior investigations of transparency have been limited to the intact lens, the outer periphery of the lens cortex [7], or to the cornea [44] with no consideration of the dense nuclear region of the lens without the complications of the cortex. We have now measured scattering for the first time using SAXS of intact slices through the lens of both the cortices and nuclei of mammalian and fish lenses. The use of fish lenses permitted investigations that served two purposes: (i) help study the effect of a relatively larger percentage (than previously investigated with mammalian systems [6,11,24]) of small monomeric particles (γ-crystallins) on the transparency and (ii) examined these considerations in lens systems (Antarctic fishes) devoid of the cold-induced LLPS or cold cataract [5].

In dilute suspensions of freely diffusing particles, density variations develop because particles will randomly and spontaneously form regions of higher and lower concentrations. Variations in particle concentration give rise to variations in index of refraction. Minor subcellular variations of the refractive index have largely been alleviated by the disintegration of most of the cellular organelles during the maturation of the crystallin-rich fiber cells [3]. Thus, it is principally the difference in index of refraction between regions of the lens where the protein concentration is above or below the mean that generate turbidity [14]. As the average particle concentration increases, there is a decreasing ability of the system to create large differences between high and low concentration regions. As a result, while the number of scattering units (particles) per unit volume grows with concentration, the ability to produce large wavelength density fluctuations drops. For systems of hard particles, the result is that the turbidity passes thought a maximum at a particle volume fraction near 0.2 and decreases with further increases in particle concentration [7].

At low protein concentrations, the intensity of scattered light grows with protein concentration. As the protein concentration increases, there is a growing probability that there exist volumes where the protein concentrations are substantially smaller or larger than the average protein volume fraction $\langle\phi\rangle$. In concentrated suspensions, the proteins pack together such that there are well-defined shells of nearest neighbors. Under these conditions, the density fluctuations occur with a periodicity on the order of a particle diameter, σ. Concentration variations with larger sizes are suppressed because there simply is no room to produce regions where the protein concentration is appreciably smaller or larger than $\langle\phi\rangle$. The result is

Please cite this article as: A.Y. Mirarefi, et al., Small-angle X-ray scattering studies of the intact eye lens: Effect of crystallin composition and concentration on microstructure, Biochim. Biophys. Acta (2010), doi:10.1016/j.bbagen.2010.02.004

that the turbidity of a colloidal suspension passes through a maximum.

Transparency in the visible region is dominated by density fluctuations with sizes on the order of the wavelength of visible light, λ_L. As $\lambda_L/\sigma >> 1$, increased transparency in dense suspensions is associated with diminished long wavelength concentration fluctuations [45]. At low concentrations, turbidity increases because the concentration of primary scattering units is increasing. However, at high concentrations, turbidity decreases due to reduced density fluctuations which results in the concentration being more uniform. These observations indicate that for a solution of proteins all the same size, as reported for γ-crystallins, there is a maximum in turbidity that occurs at a protein volume fraction, $\phi \sim 0.2$ [7].

At high loadings, local crowding results in the fluctuations in concentration that occur on a length scale of σ and thus give rise to a peak in scattering intensity near $2\pi/\sigma$. This microstructure, where each particle has well-defined shells of disordered neighbors, is referred to as liquid-like order and is the basis of transparency in eye lenses [14]. For proteins that are all the same size, the peak in scattering intensity (at $2\pi/\sigma$) and the suppression of concentration fluctuations (with wavelengths of $\sim\lambda_L$) have the same origin–crowding. For less well-defined suspensions such as the lens where the suspension is composed of particles with broad size distributions and/or mixtures of particles with different sizes, the periodicity in concentration and peaks in scattering intensity that are associated with order may not be present. However, long wavelength fluctuations can still be suppressed simply because of the effects of crowding.

These preceding arguments hold as long as the system remains in a single phase and the attractions are not so strong that the particles form essentially irreversible clusters. The temperature-induced LLPS (cold cataract) seen in mammalian eye lenses is associated with the formation of droplets of one liquid phase in the presence of a second phase [46]. It is the droplets that scatter the light and give rise to the high turbidity. If these conditions are avoided, attractions between particles can give rise to gelation. Gelation occurs when particles are localized by cages of nearest neighbors and cannot diffuse over large distances relative to their diameter [21]. In dilute suspensions, if the strength of attraction is sufficient to produce a gel, large light scattering fractal clusters are formed, and the suspension turbidity increases. However, in the case of dense suspensions, and again owing to space-filling constraints, as the overall particle concentration increases the difference in concentration between the environment outside of the clusters and within the clusters is minimized [22]. The ultimate result is that dense gelled suspensions will have a low turbidity [22,23,47,48]. This type of extreme density ($\geq 900\,\mathrm{mg\,ml^{-1}}$) of crystallins (proteins) necessary for a gelled state is often seen in the nucleus of eye lenses of the fishes as in the Antarctic toothfish, *D. mawsoni*. Eventhough the concentration of crystallins in a fish lens is twice that of the cow and the crystallins exist in a gelled state, its lens is still transparent. We hypothesize that this ultradense gelled condition is due to the suppression of the density fluctuations which leads to reduced scattering.

An alternate hypothesis or possible explanation for a loss in peak in the nucleus due to reduced scattering could be due to the severe reduction of water leading to a lack of electron contrast thus resulting in decreased X-ray scattering intensity. While we cannot discount this explanation entirely, we have investigated the water content of both the bovine and toothfish cortex and found that they have substantial water [28]. For example, the very dense toothfish lens nucleus has ~50% of its mass as water. Also, as mentioned earlier, a substantial signal (more intense than the cortex regions) was measured from the nuclear regions of the lens thus indicating that scattering was particle dominated and that the reduced contrast did not play a significant role.

4.2. Effect of polydispersity and different populations on scattered intensity

Both the lens cortices and nuclei of all species examined in this study have a low turbidity, which is obvious by their optical transparency. Thus, we may conclude that, in both regions of the lens, the protein volume fraction does not vary far from $\langle\phi\rangle$ when averaged over regions with sizes on the order of the wavelength of visible light. In the cortex of all species studied here, there is evidence of liquid-like ordering, while in the nucleus, the signature peak in scattered intensity was not observed. To understand these observations, we offer the following two hypotheses. First, as the protein in the nucleus are older, we may expect increased aggregation giving rise to a broader size distribution of the scattering entities, which indeed has been reported by a number of other investigators [2,49–51]. Such age-related aggregation has been reported for the α-crystallin isolated from nuclear regions of the cow lens [52], suggesting that in the nucleus, the protein aggregates may be larger and more polydisperse. Polydispersity can alter the local packing such that there are no regular concentration fluctuations and the peak in scattered intensity is lost. Our second hypothesis involves the ability of the increased concentration of γ-crystallins in the nucleus to fill in the holes left by the packing of the α/β_H-crystallins. This is achieved such that the periodicity in total protein concentration that would occur if only α/β_H-crystallins were present is lost and a more uniform protein concentration exists even on a length scale of the diameter of the α/β_H proteins. These two potential reasons for the lack of the peak in scattering intensity in the nuclear region are not exclusive and likely work in concert.

The two hypotheses proposed above are simple in nature in the sense that analytical expressions exist that can be used to test the predictions. It is possible to calculate the total scattered intensity for polydisperse spheres that do not interact (hard spheres) and also the intensity of binary system of hard spheres. In reality, the protein system is more complex since there are attractions between the different crystallins. To date, no simple analytical expressions exist to calculate the total scattered intensity in a multicomponent mixture, which involve attractions and hence are outside the scope of this work. In the cortex of the eye lens, one sees a peak in scattering that is primarily due to scattering from α/β_H proteins. As one moves to the nucleus, it is a known fact that the concentration of γ-crystallins increase. The simplest case is to see what happens when one increases the concentrations of particles (γ-crystallins) in the presence of α/β_H proteins without any attractions between the two and to test what effect polydispersity has on total scattering. This is the base case and one can build on the results of current work to include attractions which we feel will only amplify observed effects. Details on calculations performed to test the hypotheses are given below.

To explore the scattering properties of suspensions that are of mixed particle size, we write the total scattered intensity as:

$$I_s(q) \sim \Sigma_i \Sigma_j [\sigma_i^3 \phi_i \sigma_j^3 \phi_j f_i f_j]^{1/2} S_{ij} \tag{3}$$

where σ_i is the diameter of particle i, ϕ_i is the volume fraction of particle i, f_i is the particle form factor, and S_{ij} is the partial structure factor for particles of type i and j. The particle form factor represents the scattering from a single particle while S_{ij} represents the correlations in the center of masses of particles of types i and j [53]. In writing $I_s(q)$ in this manner, we are assuming that the contrast of particles is independent of particle size. At low angles ($q\sigma_i << 1$), f_i takes on the value of unity and in dilute conditions, $S_{ij} = 1$ for all q. Thus, because of σ_i/λ_L being much less than 1, the optical transparency of the eye lens is dominated by the small q scattering properties of the suspension.

Under dilute conditions $I_s(q=0) \sim \Sigma\Sigma(\sigma_i^3 \phi_i \sigma_j^3 \phi_j)^{1/2}$, indicating that the scattered intensity will grow with volume fraction, which in turn

Please cite this article as: A.Y. Mirarefi, et al., Small-angle X-ray scattering studies of the intact eye lens: Effect of crystallin composition and concentration on microstructure, Biochim. Biophys. Acta (2010), doi:10.1016/j.bbagen.2010.02.004

leads to an enhanced turbidity. At elevated volume fractions of a stable suspension, S_{ij} ($q=0$) decreases from unity faster than the volume fraction increases, such that $I_s(q=0)$ decreases. This results in a turbidity that decreases with increasing ϕ. As mentioned above for hard spheres (i.e., spheres that experience only volume exclusion interactions), the competition between single particle scattering and collective scattering results in a maximum in turbidity that occurs at a ϕ near 0.2.

When $q\sigma_i$ is of order unity, in dense suspensions of particles that are all the same size, we expect to see periodicity due to the liquid-like order that occurs from crowding effects. The maximum in scattered intensity from cortical regions at a $q\sim0.42$ nm^{-1} suggests that it is dominated by the α/β_H-crystallins (Figs. 1 and 2). Consistent with empirical data from previous studies on eye lenses [2,5,10,11,24], we are interested in investigating the effects of increasing polydispersity of particle size in addition to the effects of introducing small particles into a population of large particles on the scattering near $q\sim0.16$–0.5 nm^{-1}. This q range corresponds to the region where we expect to see periodic concentrations on the order of the size of the α/β_H protein aggregates.

The scattered intensity from each term in Eq. (3) scales as $(\sigma_i^3\sigma_j^3)^{1/2}$, indicating that scattering is dominated by the larger particles. While there are species and sample preparation effects on the sizes of the crystallins [25,28], we demonstrate the effects of polydispersity and increasing the concentration of the smaller particles (γ-crystallin) by making calculations of the total scattered intensity. In the calculations, we approximate the protein sizes for the α/β_H- and γ-crystallins as 16 nm (average of α and β) and 6 nm, respectively. The size of the α/β_H is at the low end of sizes reported when this fraction is isolated from lens by SEC but is consistent with the scattering peak seen in the cortex. When weighted by their relative volume fractions, the scattering will be dominated by α/β_H and β_L in the bovine lens. While in the Antarctic toothfish (*D. mawsoni*) lens, because of the depression of the β_L concentration, we expect the scattering to be dominated by the α/β_H and γ proteins. We choose to represent the scattering as that coming from binary mixtures of particles because of the availability of analytical methods for calculating S_{ij} for binary mixtures of hard spheres [53]. We follow the standard practice of accounting for polydispersity in particle size distribution through f_i while using S_{ij} for binary mixtures of hard spheres of narrow size distributions.

To demonstrate the effects of increasing the polydispersity of the particles in the lens, we model the α/β_H fraction as having a Gaussian size distribution with average radius, $\langle R\rangle=8$ nm ($R=\sigma/2$) and a standard deviation of δ where $\delta/\langle R\rangle$ (polydispersity) is varied from 0.05 to 0.25 (5–25%). Under these circumstances, we can approximate the form factor as:

$$f(q) = \int_0^\infty f_s(q)\, R^6 \frac{1}{\delta\sqrt{2\pi}} e^{-\frac{1}{2}\left(\frac{R-\langle R\rangle}{\delta}\right)^2} dR \tag{4}$$

where $f_s(q)$ is the form factor of a perfect sphere given by

$$f_s(q) = \left[\frac{3(\sin[qR]-qR\cos[qR])}{(qR)^3}\right]^2. \tag{5}$$

In applying Eq. (4), we have followed the standard approximation for particles where the size distribution is not too large such that $S_{ij}(q, \langle\phi\rangle)$ is that for uniform particles of diameter $\langle\sigma\rangle$ at a volume fraction $\langle\phi\rangle$. For our calculations, we use the solutions of Ashcroft and Langreth [53] to calculate S_{ij} for suspensions of hard spheres.

To demonstrate the effects of increasing aggregate size and polydispersity, we show (Fig. 4) the predictions of $I_s(q,\langle\phi\rangle)$ where we have increased the polydispersity of the α particles at a fixed total volume fraction ($\phi_\alpha=0.3$ and $\phi_\gamma=0.15$). The polydispersity of the γ particles is fixed at 5%. Average particle diameters of 16 nm for the α/β_H- and 6 nm for the γ-crystallins are from sizes estimated from the dominant scattering elements in the bovine eye lens. As can be seen

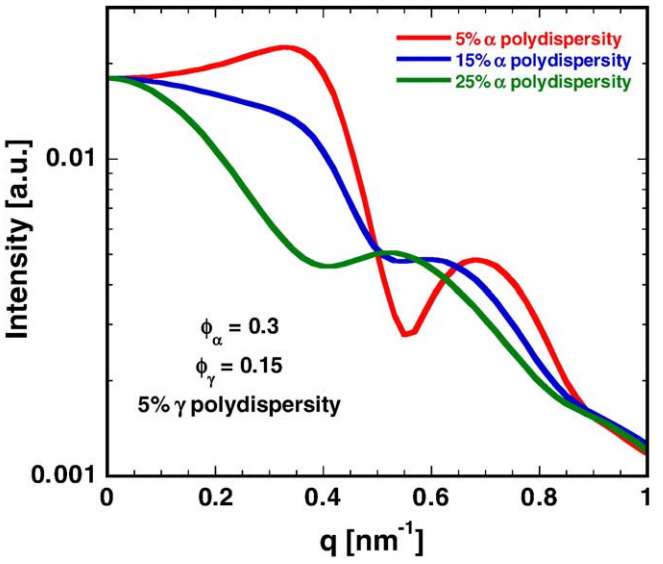

Fig. 4. Calculations of total intensity for binary mixtures of spheres with average particle diameters of 16 nm for the α/β_H and 6 nm for the γ. The volume fractions were fixed at 0.3 for the α/β_H and 0.15 for the γ. The polydispersity of the γ was fixed at 5% and the polydispersity of the α varied from 5% to 25%.

from Fig. 4, the magnitude of the first peak and subsequent oscillations in $I_s(q,\langle\phi\rangle)$ are diminished with increasing polydispersity of the α/β_H. This result suggests that even in the absence of the γ-crystallins, increased aggregation of the α/β_H and β_L proteins that leads to a larger polydispersity in size distribution can result in the loss of the peak in the scattered intensity and hence might be one of the reasons for the difference in scattering from the nucleus and the cortex. It should also be mentioned here that the effects seen (Fig. 4) of the loss in peak due to increased polydispersity of α/β_H particles is not seen if the polydispersity of γ particles is varied from 5% to 25% (at a fixed value for the α/β_H polydispersity; results not shown). This is due to the larger size of the α/β_H particles that dominate the scattering and are responsible for the observed peak (Fig. 4). Hence, variation in polydispersity of γ has a negligible effect on the scattering and the first peak.

To test the second hypothesis that the loss of the peak in scattered intensity within the lens nucleus can be attributed to the increased concentration of γ-crystallins, we plot the total scattered intensity of a binary mixture of hard spheres in which the concentration of the smaller particles (γ) is increased from near zero to a volume fraction of 0.15. This scenario can be likened to the nucleus of the eye lens in which there is an increased packing of the γ-crystallins between the α-crystallins. The volume fraction of α particles is kept fixed at 0.3 and the polydispersity of both α and γ fixed at 12.5%. As can be seen from Fig. 5, the first peak in $I_s(q,\langle\phi\rangle)$ is lost as the volume fraction of small particles increases from 0 to 0.15. The loss of this peak is an indication that there are no periodic variations in total particle density. Another effect which can be seen from this treatment (Fig. 5) is the dampening of oscillations with increasing ϕ_γ, which again suggests the loss in periodic variations of total particle density. The intensity at the low q region also decreases as more γ-crystallins are added to the system. As mentioned in the previous section, transparency in the visible region is dominated by density fluctuations with sizes on the order of the wavelength of visible light, λ_L ($q\to0$ limit). Increasing the amount of γ-crystallins reduces the amount of scattered intensity in the low q limit (Fig. 5). Thus, our hypothesis is consistent with the demonstrated suppression of density fluctuations due to increased γ-crystallin concentration. The suppression in fluctuations is seen by loss of peak in scattered intensity that gives rise to decreased scattering in the low q limit and hence an enhanced transparency in the eye lens.

Please cite this article as: A.Y. Mirarefi, et al., Small-angle X-ray scattering studies of the intact eye lens: Effect of crystallin composition and concentration on microstructure, Biochim. Biophys. Acta (2010), doi:10.1016/j.bbagen.2010.02.004

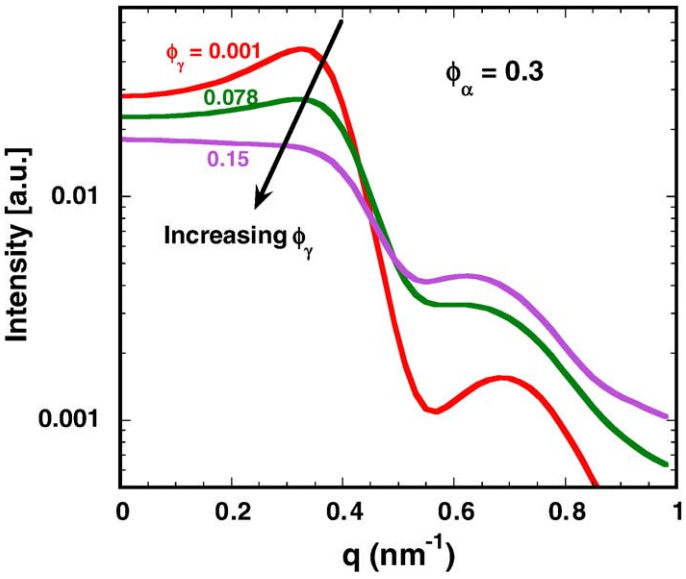

Fig. 5. Calculations of total intensity for binary mixtures of spheres with average particle diameters of 16 and 6 nm corresponding to α and γ proteins, respectively. In these calculations, a polydispersity of 12.5% is used for both α and γ proteins. Calculations are demonstrated for suspensions where the volume fraction of the large (α/β_H) particles is held constant at 0.3 while the volume fraction of the small (γ) particles increases from 0 to 0.15 corresponding to approximate changes that are anticipated in moving from the cortex to the nucleus. The main point of this figure is to illustrate the loss in peak in the scattered intensity as the concentration of γ particles increases.

A question that emerges from this hypothesis is whether the loss of the characteristic peak which indicates suppression of density fluctuations also synonymous with a loss in short-range order? To answer this question, the individual partial structure factors S_{ij}, which represent the correlations in the center of masses of particles of types *i* and *j* are given (Fig. 6). The calculations are performed with α/β_H volume fraction of 0.3 and small γ particle volume fraction of 0.15. This corresponds to the condition when the peak in scattered intensity is no longer seen (Fig. 5). The loss of the peak arises not because the large particles lose their liquid-like packing characteristics, but because $S_{\alpha\gamma}$ is negative around q^* (the position of the peak in intensity) for $S_{\alpha\alpha}$. This indicates that if one sits on a large (or α) particle, there is strong anticorrelation in locating a small (or γ) particle at a spacing corresponding to the diameter of a large particle. Fig. 6 also indicates that there is still a great deal of correlation between the centers of mass of the large and small particles. Hence short-range order still exists in the eye lenses, but a characteristic length scale for concentration fluctuations as seen from scattered intensity curves no longer exists.

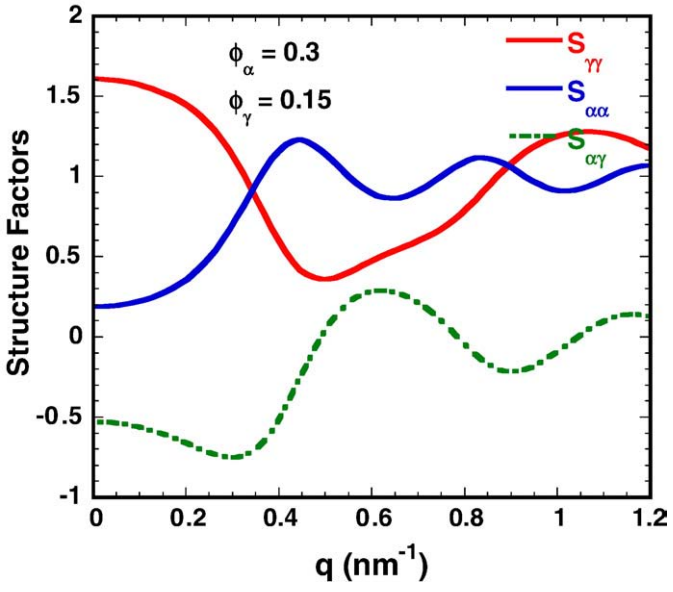

Fig. 6. Calculations of partial structure factors for the α and γ proteins as a function of waver vector q. The loss of the peak in Fig. 5 as the concentration of γ proteins increases is not because the large particles lose their liquid-like packing characteristics, but because $S_{\alpha\gamma}$ is negative around the peak position of $S_{\alpha\alpha}$. This indicates that if one sits on a large (or α) particle, there is strong anticorrelation in locating a small (or γ) particle at a spacing corresponding to the diameter of a large particle.

In conclusion, we wish to emphasize the fact that calculations of total scattered intensity of polydisperse hard spheres and binary hard sphere mixtures are representative of the base case of mixing α/β- and γ-crystallins without any attractions between the two. Just increasing the concentration of γ-crystallins (as one moves from cortex to nucleus) or changing the polydispersity of the larger α/β-crystallins (due to age related aggregation) without any added attractions is sufficient to suppress the peak in total scattered intensity. Adding attractions between the particles we feel will only amplify the observed effects. Detailed calculations of total scattered intensities with added attractions and comparisons with measured experimental data will be the basis for future work.

5. Summary and conclusions

In this report, we have described the X-ray scattering observations of the microstructure of crystallins within intact cortical and nuclear slices of the eye lens of both a terrestrial mammal and five fish species. Scattering from the cortex is characterized by a peak in scattered intensity which corresponds to a regular spacing between the α/β_H– and β_L–crystallins. This peak is associated with liquid-like ordering expected in concentrated suspensions of particles with narrow size distributions. Nuclear regions of lenses from all species investigated show no evidence of this characteristic peak seen in the cortex. We offer two hypotheses for the disappearance of the peak. The first is the increased aggregation of particles of one kind (α/β_H- and β_L-crystallins), and the second involves increased packing of γ-crystallins in the space between α- and β-crystallins. Our hypotheses are supported by model calculations of the scattered intensity of a binary suspension of hard spheres of varying polydispersity at concentrations typical of the crystallins in the nucleus. Calculations (Figs. 4 and 5) show that increasing the polydispersity of the α/β_H- and β_L-crystallins (due to aggregation) or increasing the concentration of the γ-crystallins suppresses the peak seen in the cortex. The reason behind the disappearance of the peak lies in the suppression of density fluctuations on the length scales of the large particle size—a more uniform protein concentration exists even on a length scale of the diameter of the α/β_H proteins. This situation occurs at high particle concentration for uniform (synthetic polymer systems) or even nonuniform size distribution suspensions (the lens) simply because it is not possible to generate large differences between high and low concentrations relative to the average size as the average volume fraction goes up. This hypothesis is supported by our findings in this study of the reduction of the concentration fluctuations in the lens nucleus. However, the loss in peak should not be interpreted as a loss of short-range order in the system because significant correlations still exists between the center of masses of the different species (Fig. 6). Thus, our overall conclusion is that the low turbidity of the eye lens is not the consequence of regular protein concentration variations at the length scale of a protein diameter but instead is associated with small variations from the protein concentration when averaged over volumes with sizes on the order of the wavelength of visible light. Owing to the presence of several different proteins in the eye lens, calculations performed in this work should be taken as representative of what will happen as polydispersity and relative concentrations of small and large particles change at different

Please cite this article as: A.Y. Mirarefi, et al., Small-angle X-ray scattering studies of the intact eye lens: Effect of crystallin composition and concentration on microstructure, Biochim. Biophys. Acta (2010), doi:10.1016/j.bbagen.2010.02.004

locations in the lens. Detailed calculations involving multiple particle types and interparticle interactions between different particles are required to mimic the native eye lens and remain yet to be derived. Notwithstanding these theoretical limitations, the hypotheses proposed herein are in agreement with our calculations.

Acknowledgments

The authors thank use of the Advanced Photon Source was supported by the U.S. Department of Energy, Office of Science, Office of Basic Energy Sciences, under contract no. W-31-109-ENG-38. The UNICAT facility at the Advanced Photon Source (APS) is supported by the University of Illinois at Urbana-Champaign, Materials Research Laboratory (U.S. DoE, the State of Illinois-IBHE-HECA and the NSF), the Oak Ridge National Laboratory (U.S. DoE under contract with Lockheed Martin Energy Research), the National Institute of Standards and Technology (U.S. Department of Commerce), and UOP LLC. This work was supported by the U.S. DOE via the University of Illinois at Urbana-Champaign, Frederick Seitz Materials Research Laboratory, grant no. DEFG02-96ER45439 and NSF grant OPP 02-31006 to A.L.D. and C.-H.C.C. S. Ramakrishnan would like to thank ACS-PRF for partial support (PRF no. 47954-G9).

References

[1] H. Bloemendal, The lens proteins, in: H. Bloemendal (Ed.), Molecular and Cellular Biology of the Eye Lens, Wiley & Sons, New York, 1986, pp. 1–47.
[2] H. Bloemendal, W. De Jong, R. Jaenicke, N.H. Lubsen, C. Slingsby, A. Tardieu, Ageing and vision: structure, stability and function of lens crystallins, Prog. Biophys. Mol. Biol. 86 (2004) 407–485.
[3] H. Davson, Physiology of the Eye, 5 ed.Pergamon Press, Inc., New York, NY, 1990.
[4] J.M. Dahlman, K.L. Margot, L. Ding, J. Horwitz, M. Posner, Zebrafish alpha-crystallins: protein structure and chaperone-like activity compared to their mammalian orthologs, Mol. Vis. 11 (2005) 88–96.
[5] A.J. Kiss, A.Y. Mirarefi, S. Ramakrishnan, C.F. Zukoski, A.L. Devries, C.H. Cheng, Cold-stable eye lens crystallins of the Antarctic notothenid toothfish *Dissostichus mawsoni* Norman, J. Exp. Biol. 207 (2004) 4633–4649.
[6] J.G. Sivak, The Glenn A. Fry Award Lecture: optics of the crystalline lens, Am. J. Optom. Physiol. Opt. 62 (1985) 299–308.
[7] M. Delaye, A. Tardieu, Short-range order of crystallin proteins accounts for eye lens transparency, Nature 302 (1983) 415–417.
[8] J.W. Regini, J.G. Grossmann, M.R. Burgio, N.S. Malik, J.F. Koretz, S.A. Hodson, G.F. Elliott, Structural changes in alpha-crystallin and whole eye lens during heating, observed by low-angle X-ray diffraction, J. Mol. Biol. 336 (2004) 1185–1194.
[9] J.W. Regini, K.M. Meek, Changes in the X-ray diffraction pattern from lens during a solid-to-liquid phase transition, Curr. Eye Res. 34 (2009) 492–500.
[10] W.S. Jagger, P.J. Sands, A wide-angle gradient index optical model of the crystalline lens and eye of the rainbow trout, Vision Res. 36 (1996) 2623–2639.
[11] B.K. Pierscionek, R.C. Augusteyn, The refractive index and protein distribution in the blue eye trevally lens, J. Am. Optom. Assoc. 66 (1995) 739–743.
[12] G. Wistow, K. Wyatt, L. David, C. Gao, O. Bateman, S. Bernstein, S. Tomarev, L. Segovia, C. Slingsby, T. Vihtelic, gammaN-Crystallin and the evolution of the betagamma-crystallin superfamily in vertebrates, FEBS J. 272 (2005) 2276–2291.
[13] A.J. Kiss, C.H.C. Cheng, Molecular diversity and genomic organisation of the alpha, beta and gamma eye lens crystallins from the Antarctic toothfish *Dissostichus mawsoni*, Comp. Biochem. Physiol. Pt D 3 (2008) 155–171.
[14] G. Benedek, Theory of transparency of the eye, Appl. Opt. 10 (1971) 459–473.
[15] F. Veretout, M. Delaye, A. Tardieu, Molecular basis of eye lens transparency osmotic pressure and X-ray analysis of alpha crystallin solutions, J. Mol. Biol. 205 (1989) 713–728.
[16] R.R. Ansari, K.I. Suh, S. Dunker, N. Kitaya, J. Sebag, Quantitative molecular characterization of bovine vitreous and lens with non-invasive dynamic light scattering, Exp. Eye Res. 73 (2001) 859–866.
[17] M. Delaye, A. Gromiec, Mutual diffusion of crystallin proteins at finite concentrations: a light-scattering study, Biopolymers 22 (1983) 1203–1221.
[18] M. Latina, L.T. Chylack Jr., P. Fagerholm, I. Nishio, T. Tanaka, B.M. Palmquist, Dynamic light scattering in the intact rabbit lens. Its relation to protein concentration, Invest. Ophthalmol. Vis. Sci. 28 (1987) 175–183.
[19] G. Wistow, Lens crystallins: gene recruitment and evolutionary dynamism, Trends Biochem. Sci. 18 (1993) 301–306.
[20] J.J. Wolken, Bird and fish eyes, in: J.J. Wolken (Ed.), Light Detectors, Photoreceptors, and Imaging Systems in Nature, vol. 1, Oxford University Press, New York, NY, 1995, p. 259.
[21] J.I. Clark, Order and disorder in the transparent media of the eye, Exp. Eye Res. 78 (2004) 427–432.
[22] S. Ramakrishnan, Y.L. Chen, K.S. Schweizer, C.F. Zukoski, Elasticity and clustering in concentrated depletion gels, Phys. Rev. E 70 (2004).
[23] S.A. Shah, Y.L. Chen, S. Ramakrishnan, K.S. Schweizer, C.F. Zukoski, Microstructure of dense colloid–polymer suspensions and gels, J. Phys. Condensed Matter 15 (2003) 4751–4778.
[24] B.K. Pierscionek, R.C. Augusteyn, Structure/function relationship between optics and biochemistry of the lens, Lens Eye Toxic. Res. 8 (1991) 229–243.
[25] J.S. Zigler Jr., J.B. Sidbury Jr., A comparative study of the beta-crystallins of four sub-mammalian species, Comp. Biochem. Physiol. B 55 (1976) 19–24.
[26] W. Shen, J.G. Sivak, Eyes of a lower vertebrate are susceptible to the visual environment, Invest. Ophthalmol. Vis. Sci. 48 (2007) 4829–4837.
[27] S.H. Chiou, W.C. Chang, F.M. Pan, T. Chang, T.B. Lo, Physicochemical characterization of lens crystallins from the carp and biochemical comparison with other vertebrate and invertebrate crystallins, J. Biochem. (Tokyo) 101 (1987) 751–759.
[28] A.J. Kiss, Functional, biochemical and molecular analyses of the cold stable eye lens crystallins from the Antarctic toothfish *Dissostichus mawsoni*, Ecology, Ethology & Evolution, PhD Thesis, University of Illinois at Urbana-Champaign, Urbana-Champaign, 2005, p. 184.
[29] M. Posner, A comparative view of alpha crystallins: the contribution of comparative studies to understanding function, Integr. Comp. Biol. 43 (2003) 481–491.
[30] N.J. Wagner, R. Krause, A.R. Rennie, B. Daguanno, J. Goodwin, The microstructure of polydisperse, charged colloidal suspensions by light and neutron-scattering, J. Chem. Phys. 95 (1991) 494–508.
[31] A.P. Philipse, A. Vrij, Polydispersity probed by light-scattering of secondary particles in controlled growth experiments of silica spheres, J. Chem. Phys. 87 (1987) 5634–5643.
[32] A.P. Philipse, A. Vrij, Determination of static and dynamic interactions between monodisperse, charged silica spheres in an optically matching, organic–solvent, J. Chem. Phys. 88 (1988) 6459–6470.
[33] P.N. Pusey, H.M. Fijnaut, A. Vrij, Mode amplitudes in dynamic light-scattering by concentrated liquid suspensions of polydisperse hard-spheres, J. Chem. Phys. 77 (1982) 4270–4281.
[34] A. Vrij, Concentrated, polydisperse solutions of colloidal particles—light-scattering and sedimentation of hard-sphere mixtures, J. Colloid Interface Sci. 90 (1982) 110–116.
[35] B.M. Fine, A. Lomakin, O.O. Ogun, G.B. Benedek, Static structure factor and collective diffusion of globular proteins in concentrated aqueous solution, J. Chem. Phys. 104 (1996) 326–335.
[36] A. Stradner, G. Foffi, N. Dorsaz, G. Thurston, P. Schurtenberger, New insight into cataract formation: enhanced stability through mutual attraction, Phys. Rev. Lett. 99 (2007) 198103.
[37] L. Takemoto, A. Ponce, C.M. Sorensen, Age-dependent association of gamma-crystallins with aged alpha-crystallins from old bovine lens, Mol. Vis. 14 (2008) 970–974.
[38] L.J. Takemoto, A.A. Ponce, Decreased association of aged alpha crystallins with gamma crystallins, Exp. Eye Res. 83 (2006) 793–797.
[39] A.L. DeVries, Antifreeze peptides and glycopeptides in cold-water fishes, Annu. Rev. Physiol. 45 (1983) 245–260.
[40] K.N. Holland, R.W. Brill, R.K.C. Chang, J.R. Sibert, D.A. Fournier, Physiological and behavioral thermoregulation in bigeye tuna (*Thunnus obesus*), Nature (London) 358 (6385) (1992) 410–412.
[41] A. Stradner, G. Thurston, V. Lobaskin, P. Schurtenberger, Structure and interactions of lens proteins in dilute and concentrated solutions, Progr. Colloid. Polym. Sci. 126 (2004) 173–177.
[42] S. Ramakrishnan, Y.L. Chen, K.S. Schweizer, C.F. Zukoski, Scattering studies of the structure of colloid–polymer suspensions and gels, Langmuir 19 (2003) 5128–5136.
[43] C.H. Cheng, L. Chen, Evolution of an antifreeze glycoprotein, Nature 401 (1999) 443–444.
[44] J.N. Goldman, G.B. Benedek, The relationship between morphology and transparency in the nonswelling corneal stroma of the shark, Invest. Ophthalmol. 6 (1967) 574–600.
[45] S.B. Dubin, J.H. Lunacek, G.B. Benedek, Observation of the spectrum of light scattered by solutions of biological macromolecules, Proc. Natl. Acad. Sci. U. S. A. 57 (1967) 1164–1171.
[46] M.L. Broide, C.R. Berland, J. Pande, O.O. Ogun, G.B. Benedek, Binary-liquid phase separation of lens protein solutions, Proc. Natl. Acad. Sci. U. S. A. 88 (1991) 5660–5664.
[47] A. Stradner, H. Sedgwick, F. Cardinaux, W.C.K. Poon, S.U. Egelhaaf, P. Schurtenberger, Equilibrium cluster formation in concentrated protein solutions and colloids, Nature 432 (2004) 492–495.
[48] P. Varadan, M.J. Solomon, Shear-induced microstructural evolution of a thermoreversible colloidal gel, Langmuir 17 (2001) 2918–2929.
[49] T. Kodama, R. Wong, L. Takemoto, High molecular weight aggregate from cataractous and normal human lenses: characterization by antisera to lens crystallins, Jpn. J. Opthalmol. 32 (1988) 159–165.
[50] M. Takehana, L. Takemoto, Quantitation of membrane-associated crystallins from aging and cataractous human lenses, Invest. Ophthalmol. Vis. Sci. 28 (1987) 780–784.
[51] Y. Ueda, M.K. Duncan, L.L. David, Lens proteomics: the accumulation of crystallin modifications in the mouse lens with age, Invest. Ophthalmol. Vis. Sci. 43 (2002) 205–215.
[52] B.K. Derham, J.J. Harding, alpha-Crystallin as a molecular chaperone, Prog. Retin. Eye Res. 18 (1999) 463–509.
[53] N.W. Ashcroft, D.C. Langreth, Structure of binary liquid mixtures. I, Phys. Rev. 156 (1967) 685.
[54] R.H. Kroger, M.C. Campbell, R. Munger, R.D. Fernald, Refractive index distribution and spherical aberration in the crystalline lens of the African cichlid fish *Haplochromis burtoni*, Vision Res. 34 (1994) 1815–1822.
[55] A.C. Smith, The soluble proteins in eye lens nuclei of albacore, bluefin tuna and bonito, Comp. Biochem. Physiol. B 39 (1971) 719–724.
[56] H. Fischer, I. Polikarpov, A.F. Craievich, Average protein density is a molecular-weight-dependent function, Protein Sci. 13 (2004) 2825–2828.

Please cite this article as: A.Y. Mirarefi, et al., Small-angle X-ray scattering studies of the intact eye lens: Effect of crystallin composition and concentration on microstructure, Biochim. Biophys. Acta (2010), doi:10.1016/j.bbagen.2010.02.004